Hindawi
Complexity
Volume 2022, Article ID 9350516, 16 pages
https://doi.org/10.1155/2022/9350516

Research Article

Chaotic Behaviors and Coexisting Attractors in a New Nonlinear Dissipative Parametric Chemical Oscillator

Y. J. F. Kpomahou,[1] **A. Adomou**,[2] **J. A. Adéchinan**,[3] **A. E. Yamadjako**,[4] **and I. V. Madogni**[4]

[1]*Department of Industrial and Technical Sciences, ENSET-Lokossa, UNSTIM-Abomey, Abomey, Benin*
[2]*National Higher Institute of Industrial Technology, National University of Sciences, Technologies, Engineering and Mathematics (UNSTIM) of Abomey, Abomey, Benin*
[3]*Department of Physics, FAST-Natitingou, UNSTIM-Abomey, Abomey, Benin*
[4]*Department of Physics, University of Abomey-Calavi, Abomey-Calavi, Benin*

Correspondence should be addressed to Y. J. F. Kpomahou; fkpomahou@gmail.com

Received 29 October 2021; Revised 1 December 2021; Accepted 28 February 2022; Published 21 March 2022

Academic Editor: Jesus M. Munoz-Pacheco

In this study, complex dynamics of Briggs–Rauscher reaction system is investigated analytically and numerically. First, the Briggs–Rauscher reaction system is reduced into a new nonlinear parametric oscillator. The Melnikov method is used to derive the condition of the appearance of horseshoe chaos in the cases $\omega = \Omega$ and $\omega \neq \Omega$. The performed numerical simulations confirm the obtained analytical predictions. Second, the prediction of coexisting attractors is investigated by solving numerically the new nonlinear parametric ordinary differential equation via the fourth-order Runge–Kutta algorithm. As results, it is found that the new nonlinear chemical system displays various coexisting behaviors of symmetric and asymmetric attractors. In addition, the system presents a rich variety of bifurcations phenomena such as symmetry breaking, symmetry restoring, period doubling, reverse period doubling, period-m bubbles, reverse period-m bubbles, intermittency, and antimonotonicity. On the contrary, emerging chaotic band attractors and period-1, period-3, period-9, and period-m bubbles routes to chaos occur in this system.

1. Introduction

Nonlinear oscillations remain up to now an attractive topic of research due to their applications to physics, biology, chemistry, and engineering [1–4]. To that end, various analytical methods and numerical tools have been proposed and successfully used in study of nonlinear dynamics of oscillatory systems [4–10]. Recently, nonlinear chemical oscillations have received attention of many researchers from theoretical and experimental point of view [11–27]. This is due to dynamic complexities that can exhibit the new nonlinear chemical oscillators and their potential applications in engineering. For example, Cassani et al. [19] studied the nonlinear behavior of Belousov–Zhabotinsky-type reactions focusing on modeling under different operating conditions, from the simplest to the most widely applicable models. The stability analysis of simplified models as a function of bifurcation parameter has been studied. Adéchinan et al. [20] studied the dynamics and active control of chemical oscillations governed by a forced generalized Rayleigh oscillator. The condition of the appearance of chaos has been derived using the Melnikov method. The control efficiency has been shown through the control gain parameter on the behavior of the system. Monwanou et al. [21] investigated the effect of an amplitude modulated excitation on the nonlinear dynamics of reactions between four molecules. The stability analysis of the autonomous system has been made in detail. The dynamics of the nonautonomous chemical system showed various routes to chaos. Olabodé et al. [22] used the Melnikov method and derived analytically the domains boundaries where horseshoe chaos appears in chemical oscillations. They afterward controlled

chaotic oscillations by subjecting the nonlinear chemical system to fluctuation hydrodynamic drag forces. On the contrary, the effects of passive hydrodynamics force on harmonic and chaotic oscillations in nonlinear chemical oscillations governed by a forced modified Van der pol–Duffing oscillator have been analyzed by Olabodé et al. [23]. Recently, Ghosh and Ray [24] showed that a class of arbitrary, autonomous kinetic equations in two variables, describing chemical and biochemical oscillations, can be reduced to the form of a Liénard oscillator. Binous and Bellagi [25] studied various important aspects of nonlinear dynamics such as limit cycles, quasi-periodic and chaotic behaviors, time series and phase portraits, power spectra, the time-delay reconstruction diagrams, Hopf bifurcation, bifurcation diagrams, steady-state multiplicity of four problems drawn from the chemical, and biochemical engineering field of study. Shabunin et al. [26] modeled chemical reactions by the forced limit-cycle oscillator and studied synchronization phenomena and transition to chaos.

The most theoretical studies on nonlinear dissipative chemical systems in general and on Briggs–Rauscher reaction system in particular have been performed with periodically external excitation [20, 22, 23, 27]. However, the aspects of nonlinear dynamics of Briggs–Rauscher reaction system under the influence of the parametric and two external periodic excitations have not been yet studied. Such a study will be important to perform since it is well known that the dynamics of a nonlinear system subjected to parametric and external excitations exhibits complex and rich dynamical behaviors [9, 28–30]. Thus, the problem of interest is to show that the Briggs–Rauscher reaction system can be modeled by the following new nonlinear parametric oscillator:

$$\begin{aligned} &x + \mu\left(1 + x^2 + p\gamma\cos\omega t\right)\dot{x} \\ &\quad + (1 + p\cos\omega t)\left(\alpha_1 x + \alpha_3 x^3\right) \\ &\quad = -\alpha_0\,(1 + p\cos\omega t) + f\cos\Omega t, \end{aligned} \tag{1}$$

where the dots indicate differentiation with respect to time t and μ, p, α_i f, ω, and Ω are real system parameters.

The originality of this work is brought by the parameter p which controls the presence of the parametric and external excitations of frequency ω. It is important to point out that Si-yu and Jin-yan [29] considered a particular case of this strong nonlinear parametric equation in the study of the parameter stability and global bifurcations. It is now easy to see through this equation that when $p = 0$, the classical nonautonomous Van der Pol–Duffing oscillator is obtained. This classical driven oscillator has been widely studied in the context of various physical, chemical, and engineering problems. Some theoretical and numerical results for some particular cases of the strong nonlinear parametric system (1) have been found in the open literature. Therefore, the dynamics study of system (1) is of a crucial importance in nonlinear chemical oscillations for a better understanding of the dynamical behaviors of the system. In addition, the investigation of nonlinear phenomena in dynamical system (1) is even significance in practical applications.

In order to predict the chaotic behavior in a driven nonlinear system, the Melnikov theory is often used [9, 27, 42]. From this theory, the condition for the existence of homoclinic bifurcation to occur in the case where the potential is an asymmetric or symmetric double well exists in the open literature for $p = 0$. However, for $p \neq 0$, the prediction of horseshoe chaos in a new nonlinear parametric system (1) under two periodic external excitations has not been investigated up to now. Thus, the presence of the parameter p would contribute to nonlinear dynamics of Briggs–Rauscher reaction system modeled by equation (1).

The coexisting attractors exist in many natural and artificial systems. This phenomenon has received the attention of many investigators in nonlinear dynamics fields [13, 20, 21, 31]. This is due to the fact that it provides multiple optional steady states for the system to respond to different needs. To that end, various studies on some driven nonlinear systems have shown the existence of multiple coexisting attractors [32–39]. In nonlinear chemical dynamics, the coexistence of two or more stable dynamical states (steady state, periodic oscillation, and chaos) of a system, under the same set of external constraints-input concentration of reactants, temperature, pressure, and so on, is one of the most interesting and significant phenomena. Although the coexistence of attractors offers important advantages to systems to respond to different solicitations, it also affects the performance of the system to some extent. For this reason, its prediction is become a necessity for the scientific community in recent years. Therefore, the study of coexisting of symmetric and asymmetric attractors in a new parametric chemical oscillator described by (1) is of fundamental and even practical interest. Furthermore, the prediction of coexisting attractors in a Briggs–Rauscher reaction system modeled by a strong nonlinear oscillator with damping and stiffness time-varying described by (1) has not yet been studied. So, the second problem that attracts our attention in this work is the prediction of chaos and coexisting attractors in a new nonlinear parametric chemical system governed by equation of motion (1).

In order to attain our objective, we firstly show that the Briggs–Rauscher kinetic equations can be reduced to a new nonlinear parametric oscillator given by equation (1), and we apply the Melnikov method for deriving the condition of the appearance of horseshoe chaos (Section 2). Second, we investigate the existence of coexisting of attractors by solving numerically the equation of motion (1) via the fourth-order Runge–Kutta algorithm (Section 3). Finally, we end with a conclusion (Section 4).

2. Mathematical Model and Melnikov Analysis

2.1. Mathematical Model. We consider in this work the Briggs–Rauscher reaction system [40] which represents a simple model for designing a chemical oscillator. Such a

reaction was proposed by Boissonade and de Kepper [41]. The governing equations are defined as follows:

$$\begin{aligned} \dot{u} &= -u^3 + \mu_0 u - kv - \lambda, \\ \dot{v} &= \frac{1}{s}(u - v), \end{aligned} \tag{2}$$

where μ_0 and k are the positive parameters, s is the characteristic evolution time of the feedback $-kv$, and λ is here considered as constant negative feedback for the system. In theoretical studies performed up to now, system (2) has been transformed into a Liénard-type oscillator by considering s as a constant parameter [20, 22–24, 27]. The novelty of this work constitutes to express the characteristic evolution time s under the following form:

$$s^{-1} = s_0^{-1}(1 + p\cos\omega t). \tag{3}$$

By differencing the first equation of system (2) and taking into account its second equation and equation (3), we obtain after some mathematical manipulations the following equation:

$$\begin{aligned} &x + \mu\left(1 + x^2 + p\gamma\cos\omega t\right)\dot{x} \\ &+ (1 + p\cos\omega t)\left(\alpha_1 x + \alpha_3 x^3\right) \\ &= -\alpha_0(1 + p\cos\omega t), \end{aligned} \tag{4}$$

where $\mu = (1/s_0) - \mu_0$, $\alpha_0 = (\lambda/s_0)\sqrt{(3/\mu)}$, $\alpha_1 = (k - \mu_0)/s_0$, $\alpha_3 = (\mu/3s_0)$, $\gamma = 1/s_0\mu$, $A = \sqrt{3s_0/(\mu_0 s_0 - 1)}$, and $u = (1/A)x$.

Now, taking into account the influence of the external excitation of the form $g\cos\Omega t$, we finally obtain the desired equation of motion (1). It is easy to see that when $p = 0$, a similar equation (1) has been used to describe the nonlinear chemical oscillations of Briggs–Rauscher reaction system [22, 27]. After establishment of the equation of motion (1), we use in the next section the Melnikov method for deriving the condition of the appearance of horseshoe chaos in the cases, where $\omega = \Omega$ and $\omega \neq \Omega$.

2.2. Melnikov Analysis. The Melnikov method is a powerful analytical tool widely used to predict the existence of horseshoe chaos in a nonautonomous system [9, 27, 42]. In order to perform such a prediction, we rewrite (1) under the form of a first ordinary differential equation, that is,

$$\begin{aligned} \dot{x} &= y, \\ \dot{y} &= -\alpha_0 - \alpha_1 x - \alpha_3 x^3 - \varepsilon\mu\left(1 + x^2 + p\gamma\cos\omega t\right)y \\ &\quad - \varepsilon p\left(\alpha_0 + \alpha_1 x + \alpha_3 x^3\right)\cos\omega t + \varepsilon f\cos\Omega t, \end{aligned} \tag{5}$$

where ε is a small perturbation quantity, that is, $0 < \varepsilon < 1$. From the system of (5), the unperturbated system obtained with $\varepsilon = 0$ becomes

$$\begin{aligned} \dot{x} &= y, \\ \dot{y} &= -\alpha_0 - \alpha_1 x - \alpha_3 x^3. \end{aligned} \tag{6}$$

System (6) is Hamiltonian, and the potential function and associated Hamiltonian are

$$\begin{aligned} V(x) &= \alpha_0 x + \frac{1}{2}\alpha_1 x^2 + \frac{1}{4}\alpha_3 x^4, \\ H(x, y) &= \frac{1}{2}y^2 + V(x), \end{aligned} \tag{7}$$

respectively. The homoclinic orbits corresponding to system (6) are given by the following expressions [27]:

$$\begin{aligned} x_h &= x_0 + \frac{\sqrt{2}\sigma^2}{\alpha_3\left(x_0 \pm \delta\cosh\sigma\tau\right)}, \\ y_h &= \mp\frac{\sqrt{2}\delta\sigma^3\sinh(\sigma\tau)}{\alpha_3\left(x_0 \pm \delta\cosh(\sigma\tau)\right)^2}, \end{aligned} \tag{8}$$

where $x_0 = \alpha_0/2\alpha_1\sqrt{-3\alpha_3/\alpha_1}$, $\delta^2 = -\alpha_1/\alpha_3 - 1/2x_0^2$, $\sigma^2 = -\alpha_1 - 3/2\alpha_3 x_0^2$, $\tau = t - t_0$, and t_0 is the cross-section time of the Poincaré and can be considered as the initial time of the forcing time. When $\varepsilon \neq 0$, the Melnikov method can be applied. Thus, the Melnikov integral function is defined as follows:

$$\begin{aligned} M(t_0) = -\mu\Big(&\int_{-\infty}^{+\infty} y_h^2 \mathrm{d}\tau + \int_{-\infty}^{+\infty} x_h^2 y_h^2 \mathrm{d}\tau\Big) \\ &- \frac{p}{s_0}\int_{-\infty}^{+\infty} y_h^2\cos(\omega t)\mathrm{d}\tau - p\alpha_1\int_{-\infty}^{+\infty} x_h y_h\cos(\omega t)\mathrm{d}\tau \\ &- p\alpha_3\int_{-\infty}^{+\infty} x_h^3 y_h\cos(\omega t)\mathrm{d}\tau - p\alpha_0\int_{-\infty}^{+\infty} y_h\cos(\omega t)\mathrm{d}\tau \\ &+ f\int_{-\infty}^{+\infty} y_h\cos(\Omega t)\mathrm{d}\tau. \end{aligned} \tag{9}$$

Taking into consideration the expressions of the quantities x_h and y_h given by (8) and using the standard integral table [43], the Melnikov integral function (9) yields after some mathematical manipulations to the following equation:

$$M(t_0) = K_0 + pK_1\cos(\omega t_0) + pK_2\sin(\omega t_0) + fK_3\sin(\Omega t_0). \tag{10}$$

Assuming that $\Omega = \omega$, the Melnikov function (10) becomes

$$M(t_0) = K_0 + pK_1\cos(\omega t_0) + (pK_2 + fK_3)\sin(\omega t_0), \tag{11}$$

where the expression of K_i, $i = \overline{0, 3}$, are given in Appendix. It is easy to remark that (11) can be rewritten as follows:

$$M(t_0) = K_0 + \sqrt{K_1^2 p^2 + (K_2 p + K_3 f)^2}\cos(\omega t_0 - \phi), \tag{12}$$

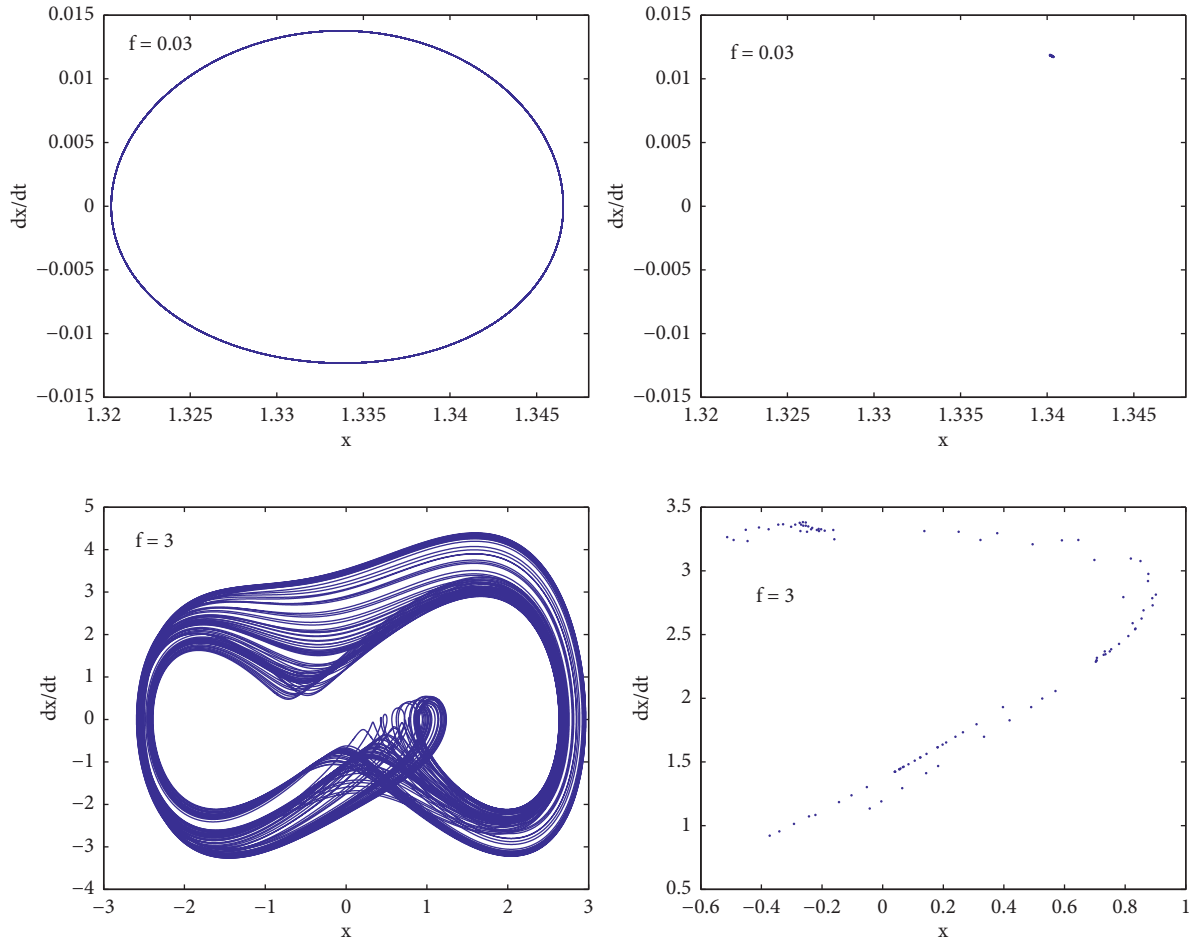

Figure 1: Phase portraits and its corresponding Poincaré maps showing the validation of the proposed analytical prediction of horseshoe chaos in the case $\omega = \Omega$.

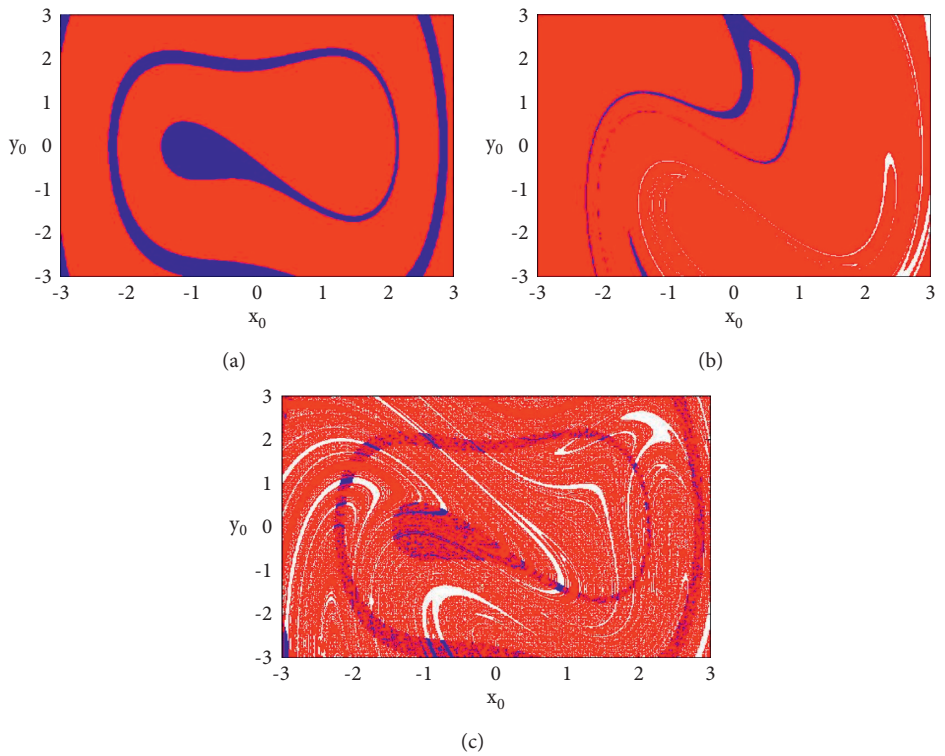

Figure 2: Basins of attraction of the new parametric chemical system (1) with the parameters of Figure 1 for three different values of f: (a) $f = 0.03$, (b) $f = 2$, and (c) $f = 3$.

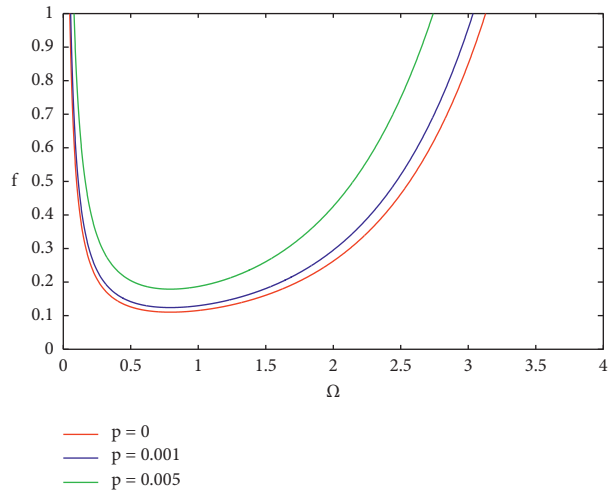

Figure 3: Melnikov threshold curves for homoclinic chaos in the (f, Ω) plane with $\omega = (\sqrt{5} - 1)/2$ and for three different values of p. The other parameters of Figure 1 are kept constant.

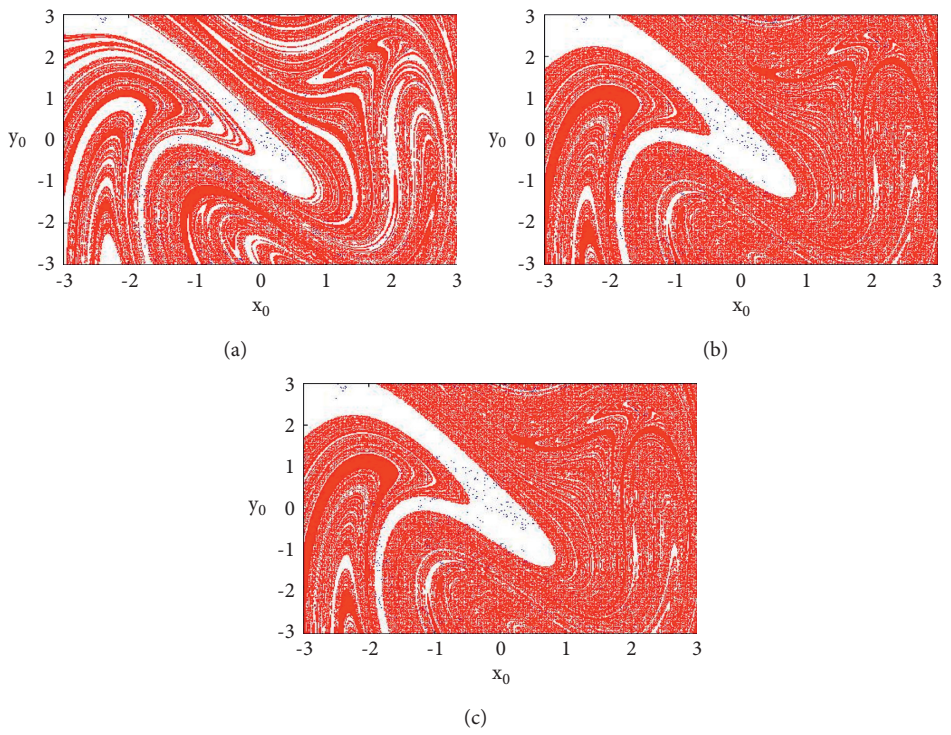

Figure 4: Basins of attraction of the new parametric chemical system (1) showing the effect of p with the parameters of Figure 3 for $\omega = (\sqrt{5} - 1)/2$ and $\Omega = 1$: (a) $p = 0$, (b) $p = 0.001$, and (c) $p = 0.05$.

with $\phi = \arctan(K_2 p + K_3 f / K_1 p)$.

To determine the Melnikov criterion for appearance of horseshoe chaos in our new nonlinear dissipative parametric oscillator, it is necessary to let $M(t_0) = 0$ with $M'(t_0) \neq 0$. Thus, $M(t_0) = 0$ leads to

$$\cos(\omega t_0 - \phi) = -\frac{K_0}{\sqrt{K_1^2 p^2 + (K_2 p + K_3 f)^2}}. \tag{13}$$

Since $M'(t_0) = -\omega\sqrt{K_1^2 p^2 + (K_2 p + K_3 f)^2}\sin(\omega t_0 - \phi) \neq 0$ implies $\sin(\omega t_0 - \phi) \neq 0$, then $\cos(\omega t_0 - \phi) \neq 0$. Thus, $|\cos(\omega t_0 - \phi)| < 1$. Therefore, the condition for the existence of chaos is obtained if

$$M_1 = \left|\frac{K_0}{\sqrt{K_1^2 p^2 + (K_2 p + K_3 f)^2}}\right| < 1. \tag{14}$$

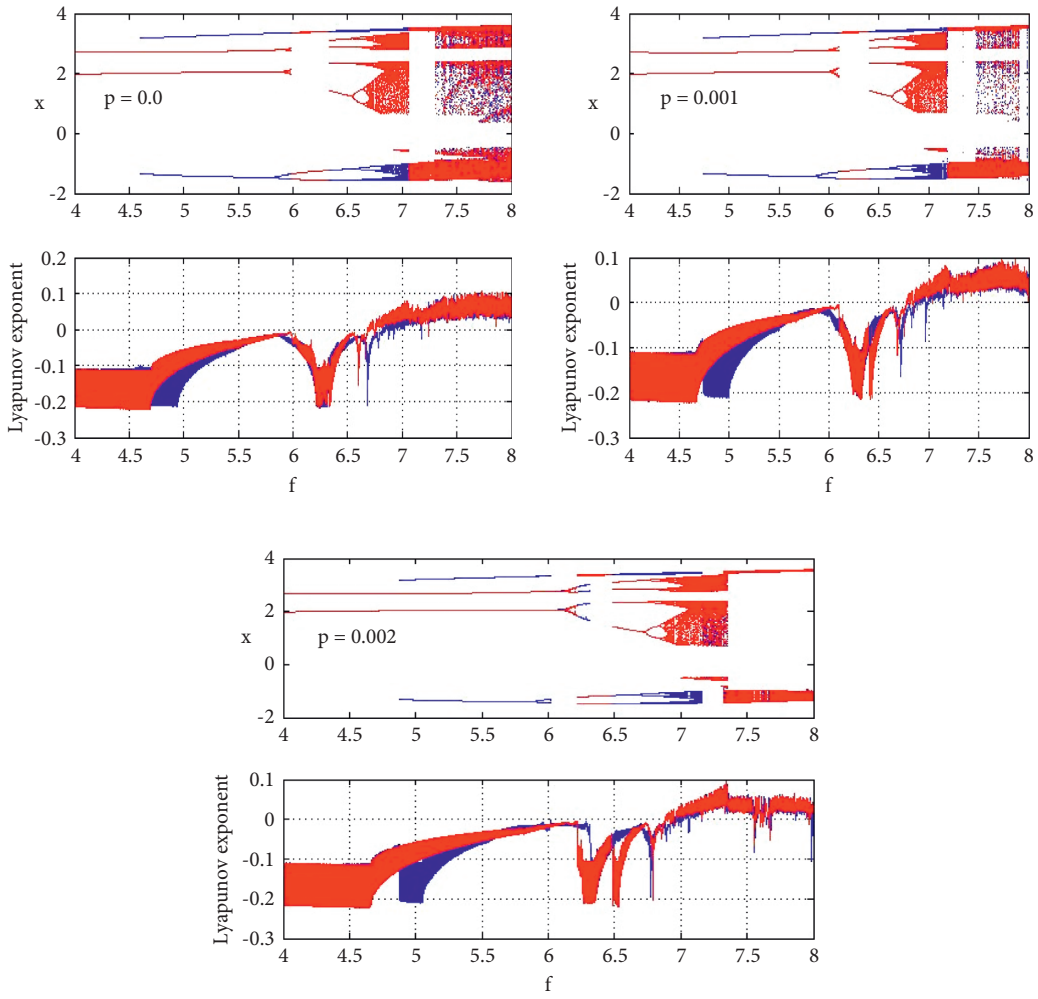

Figure 5: Bifurcation diagrams and its corresponding Lyapunov exponents vs. f exhibiting the effect of p with the parameters of Figure 1.

From this analytical result, the following theorem can be formulated.

Theorem 1. *If condition (14) is verified, then a homoclinic bifurcation occurs and the new parametric chemical system (1) may exhibit chaotic behavior.*

Using the following system parameters $k = 25.361$, $\mu_0 = 25.41$, $s_0 = 0.0392$, $\lambda = -0.0025$, $\omega = \Omega = 1.0$, and $p = 0.001$, we obtain $M_1 > 1$ for $f = 0.03$ and $M_1 < 1$ for $f = 3$. Therefore, the desired system given by (1) may display periodic motion for $f = 0.03$. However, when $f = 3$, the new chemical system (1) may exhibit chaotic behavior. The numerical simulations realized in Figure 1 under initial conditions $x(0) = 0.5$ and $\dot{x}(0) = 0.5$ confirm the analytical prediction. To test again the validity of the proposed analytical prediction, we have plotted in Figure 2, the basins of attraction of the new nonlinear chemical system (1) which represent a best tool to study numerically the regularity or irregularity of the attractors. These basins of attraction are obtained by solving numerically the equation of motion (1) and collecting the initial conditions for which the dynamics of the new chemical system is sensitive. From Figure 2(a), we obtain that the new parametric chemical oscillator show a regular behavior when $f = 0.03$. However, the erosion of the basin of attraction appears and becomes more and more visible for $f = 2$ and $f = 3$. Thus, we can conclude that the analytical and numerical results are in good agreement.

Now, in the case where $\omega \neq \Omega$, the Melnikov function (10) becomes

$$M(t_0) = K_0 + p\sqrt{K_1^2 + K_2^2}\sin(\omega t_0 + \psi) + fK_3 \sin \Omega t_0, \tag{15}$$

with $\tan \psi = K_1/K_2$. For $p \neq 0$ and $\omega \neq \Omega$, the condition of a zero of this Melnikov function is obtained from $|\sin(\omega t_0 + \psi)| < 1$ and $|\sin(\Omega t_0)| < 1$. Therefore, a sufficient condition for the onset of Melnikov chaos in our new chemical system (1) can be expressed from [44, 45] as follows:

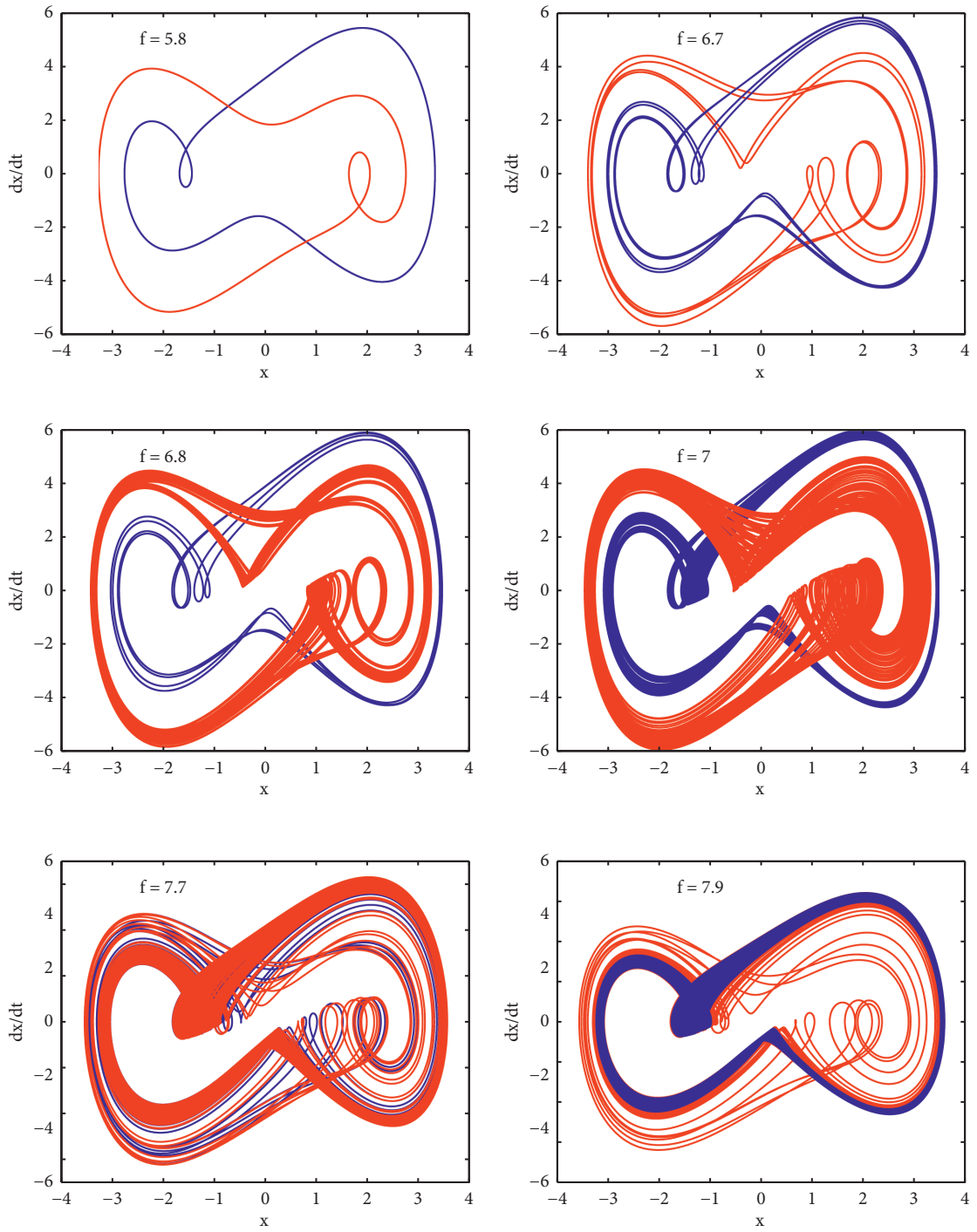

Figure 6: Various phase portraits illustrating the coexistence of two attractors for different values of f with the parameters of Figure 5.

$$f \geq \left| \frac{p\sqrt{K_1^2 + K_2^2} - K_0}{K_3} \right|. \tag{16}$$

From (16), the following theorem can be formulated.

Theorem 2. *If condition (16) is satisfied, then a homoclinic bifurcation occurs and the new chemical system (1) may display chaotic motion.*

Figure 3 shows the dependence of the amplitude f of the periodic external excitation on the frequency Ω for three different

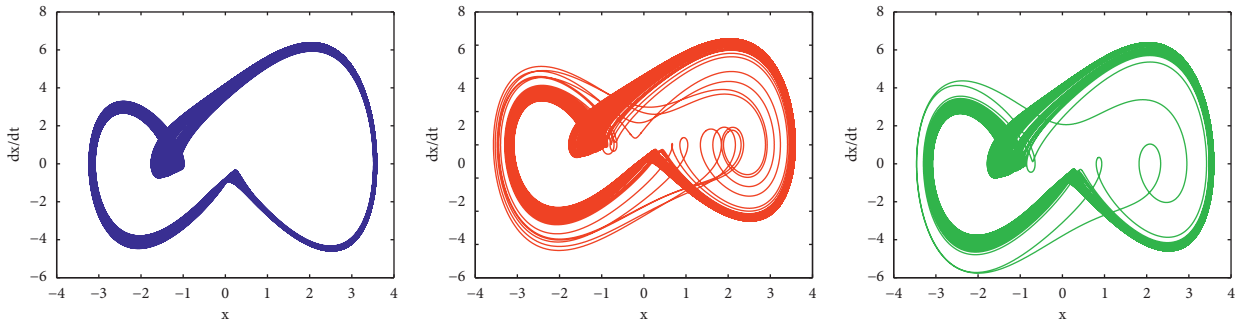

FIGURE 7: Phase portraits showing the coexistence of three different chaotic attractors for $f = 7.9$ under three initial conditions: (a) (0.5, 0.5), (b) (−0.5, −0.5), and (c) (−0.8, 0).

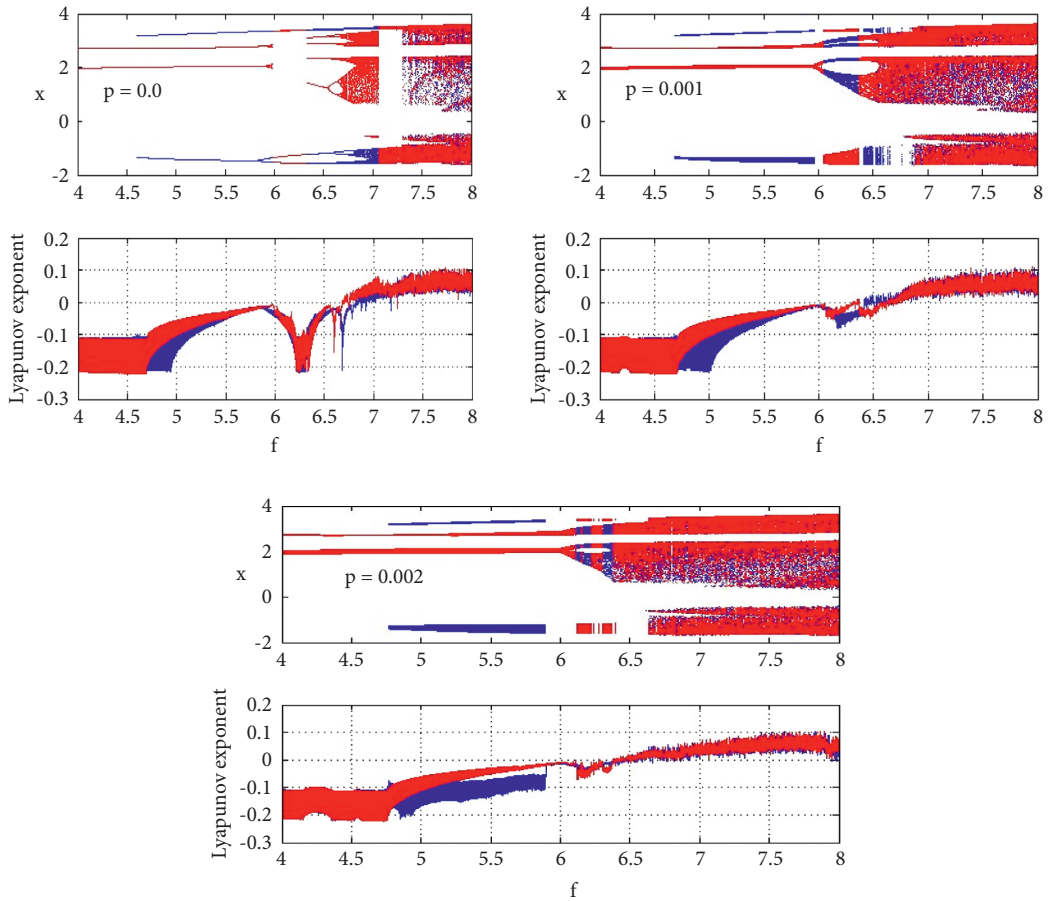

FIGURE 8: Bifurcation diagrams and its corresponding Lyapunov exponents versus f showing the effect of p when $\omega = (\sqrt{5} - 1)/2$ and $\Omega = 1$. The parameters of Figure 3 are kept constant.

values of p. Through this figure, we notice that the horseshoe chaos region decreases when p increases. This observation is confirmed by the basins of attraction shown in Figure 4.

3. Coexisting Attractors

The aim of this section is to investigate the coexisting behaviors of attractors and the eventual transitions to chaos that can arise in the Biggs–Rauscher (BR) reaction system governed by equation of motion (1) when the parameter p varies. For this, we solve numerically the equation of motion (1) by using the fourth-order Runge–Kutta algorithm with the following system parameters: $k = 25.361$, $\mu_0 = 25.41$, $s_0 = 0.0392$, and $\lambda = -0.0025$. The initial conditions and the calculation step used to realize the numerical simulations are (0.5, 0.5) (blue color), (−0.5, −0.5) (red color), (−0.8, 0.0) (green color), (0.2, 0.2) (yellow color), and $h = 0.005$, respectively.

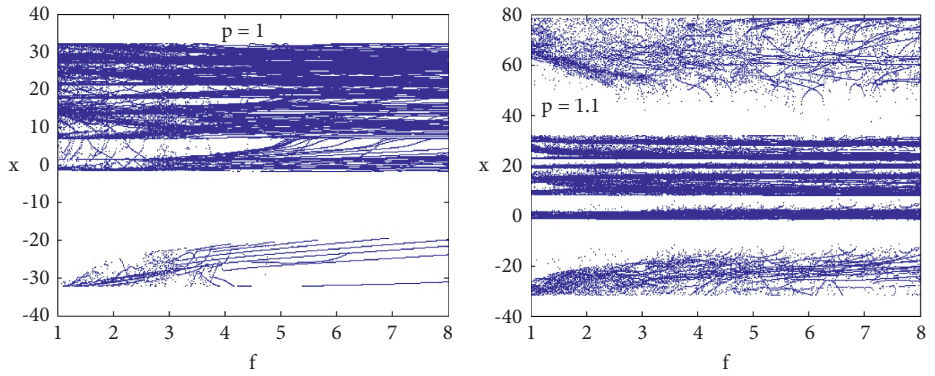

Figure 9: Effect of p on the bifurcation diagrams of the new nonlinear parametric chemical system (1) with the parameters of Figure 8.

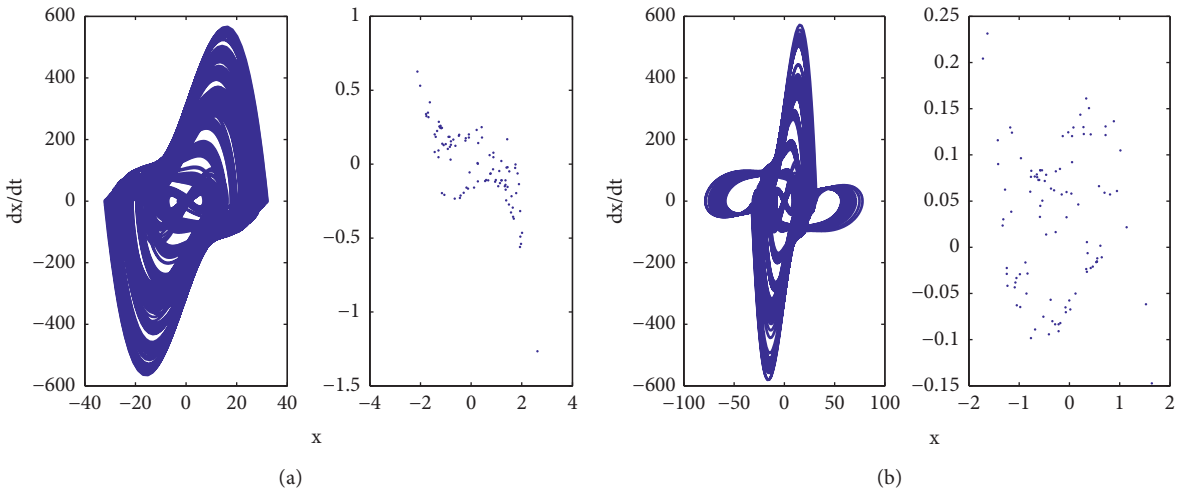

Figure 10: Phase portraits and its corresponding Poincaré maps illustrating the chaotic behavior of the new chemical system (1) with the parameters of Figure 9 for (a) $f = 3$, $p = 1.0$ and (b) $f = 1.8$, $p = 1.1$.

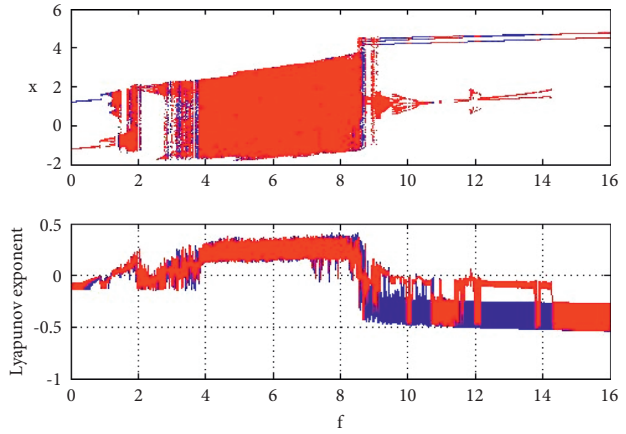

Figure 11: Bifurcation diagrams and its corresponding Lyapunov exponents with $\alpha_0 = -0.0193$, $p = 0.005$, $\omega = 1$, and $\Omega = 3$. The other system parameters are fixed.

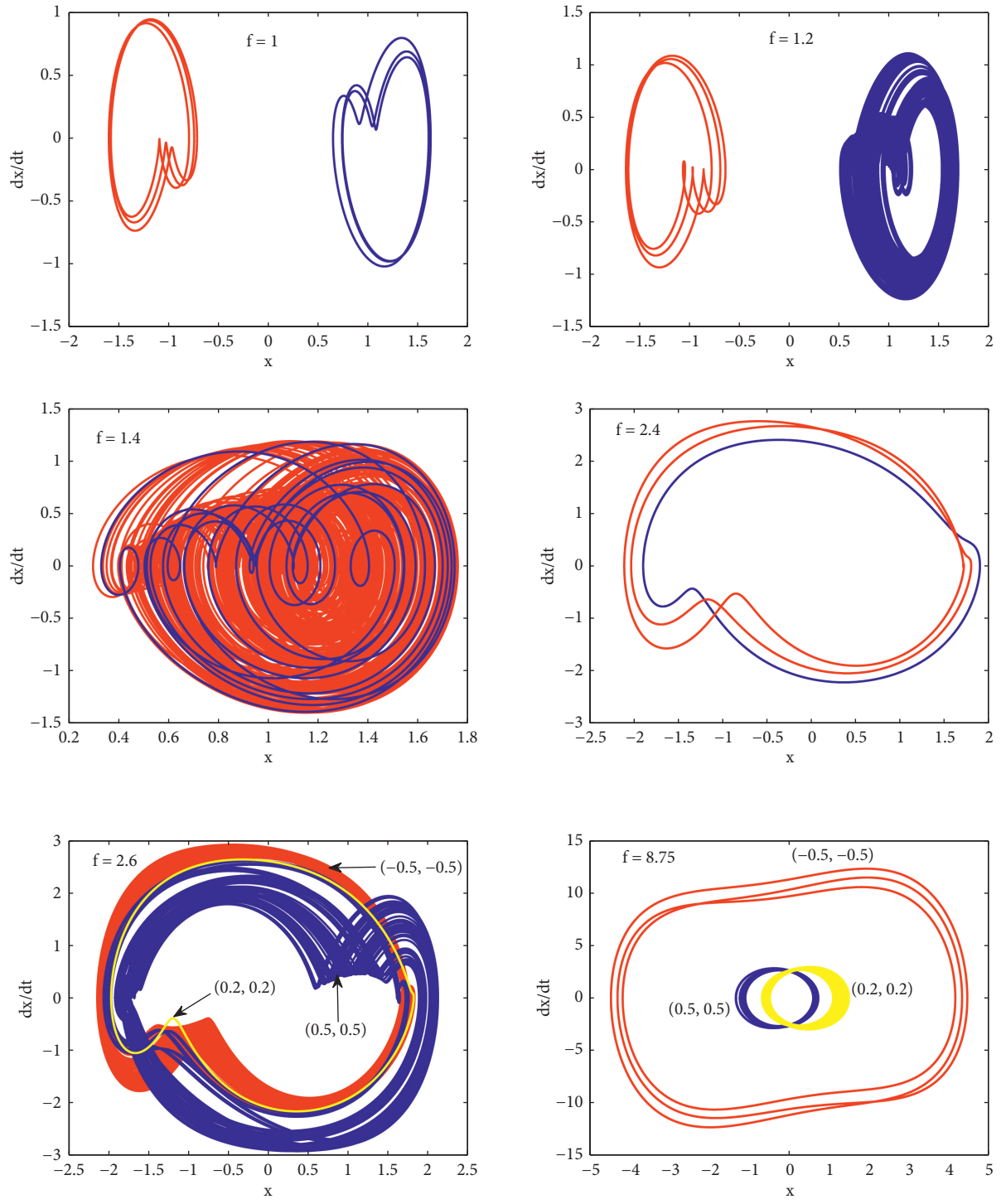

FIGURE 12: Coexisting behaviors of attractors in a new parametric chemical system (1) with $\Omega = 3$, $\omega = 1$, $p = 0.005$, and $\alpha_0 = -0.0193$. The other system parameters are kept constant.

Figure 5 shows the influence of p on the bifurcation diagrams of Biggs–Rauscher (BR) reaction system described by equation (1). Through this figure, we notice that this parameter accentuates the symmetry breaking phenomenon and removes the symmetry restoring phenomenon. Moreover, the coexistence of attractors

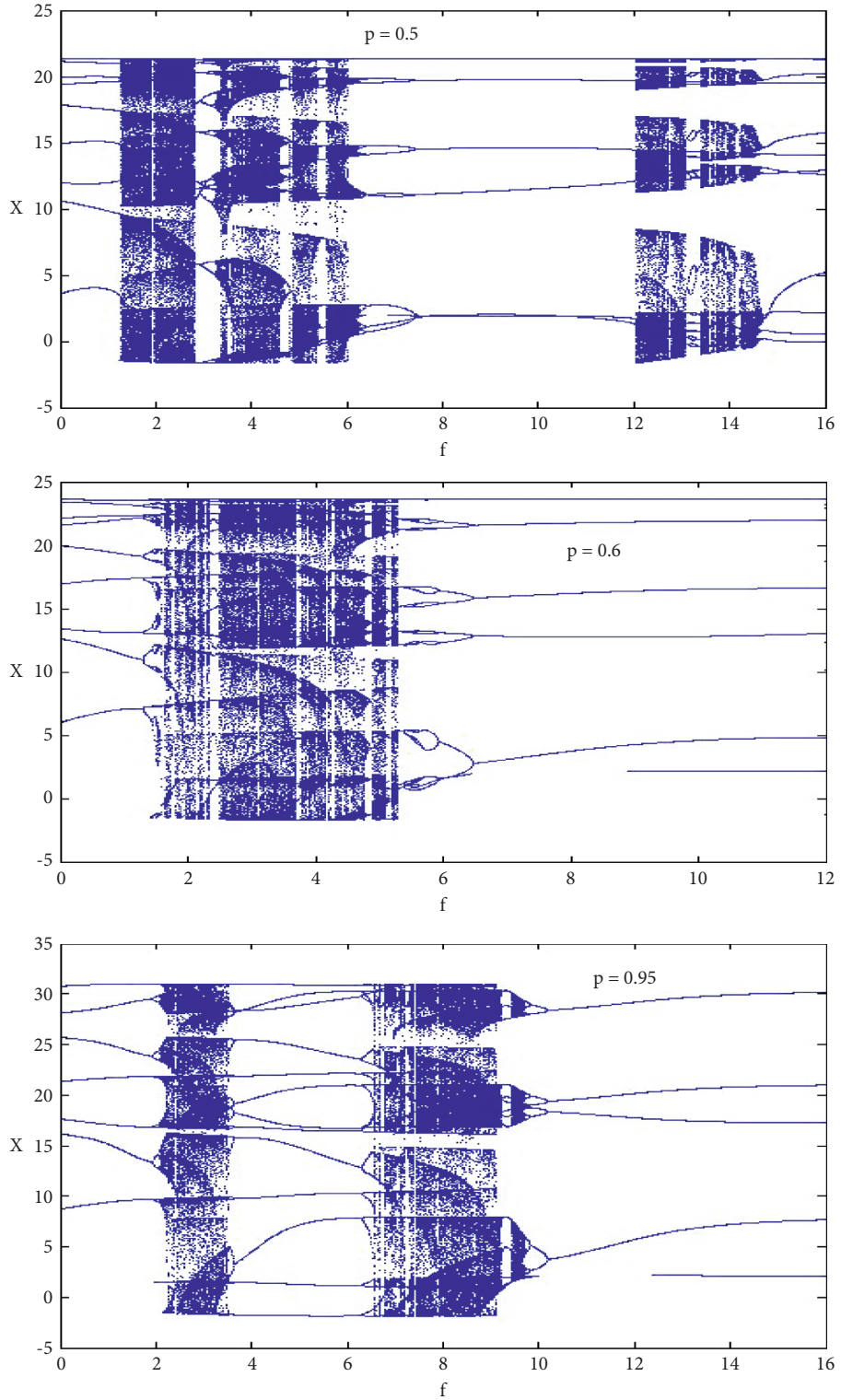

Figure 13: Effect of p on the bifurcation diagram of Figure 11 of the new chemical system obtained under initial conditions (0.5, 0.5).

remains in the system under the study when $p \neq 0$. Figure 6 illustrates the coexisting behaviors of attractors for several different values of f for $p = 0.001$. From this figure, we clearly see that the new nonlinear dissipative parametric chemical system presents multiple coexisting attractors. For example, when $f = 5.8$, the left period-2 orbit coexists

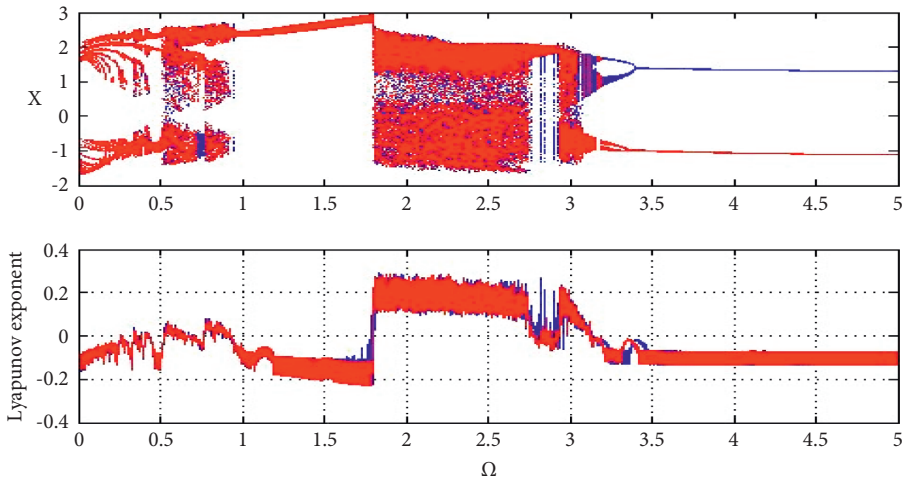

Figure 14: Bifurcation diagrams and its corresponding Lyapunov exponents vs. Ω with $f = 1.8$, $\alpha_0 = -0.0193$, and $p = 0.005$ The other parameters are kept constant.

with the right period-2 orbit. For $f = 6.7$, asymmetric period-6 and period-8 orbits coexist. As $f = 6.8$, the left period-6 orbit coexists with the right chaotic attractor. When $f = 7$, two chaotic asymmetric attractors of different topologies coexist. On the contrary, chaotic symmetric attractors of different complexities coexist when $f = 7.7$ and $f = 7.9$. In addition, we found that, for $f = 7.9$, the new parametric chemical system (1) displays with three different initial conditions and chaotic behaviors of different topologies (see Figure 7).

We have afterward analyzed the influence of the parameter p on the bifurcation diagrams of the chemical reaction system under consideration when $\omega \neq \Omega$. Thus, by keeping constant the other parameters and taking $\omega = (\sqrt{5} - 1)/2$ and $\Omega = 1$, the obtained results are shown in Figure 8. From this figure, we notice that the presence of the parameter p provokes always a symmetry breaking. In addition, the geometrical shape of attractors is modified, and we note the disappearance of the symmetry restoring crisis phenomenon. For $p = 1.0$ and $p = 1.1$, the bifurcation structures have completely changed, as shown in Figure 9. In addition, we clearly see through this figure that the amplitude of oscillations becomes important. In order to have an idea about the new chemical system behavior as predicted by these bifurcation diagrams, two phase portraits and its corresponding Poincaré maps are plotted in Figure 10 for two values of f. Through this figure, we notice that the new parametric chemical system (1) exhibits for these chosen system parameters and chaotic behaviors which are confirmed by the Poincaré maps. When ω/Ω is rational, that is, $\omega = 1$ and $\Omega = 3$, the new parametric chemical system (1) displays bistability phenomenon, symmetric coexisting attractors, and asymmetric coexisting attractors (see Figure 11). The coexisting behaviors of asymmetric attractors of different topologies are illustrated in Figure 12. We also notice that, for $f = 2.6$, two chaotic symmetric attractors of different complexities coexist with a period-1 orbit. Moreover, when $f = 8.75$, two asymmetric quasi-periodic orbits coexist with a period-3 orbit of large oscillation amplitude. We have also investigated, in this case of oscillation, the effect of p on the bifurcation diagram of Figure 11 obtained with initial conditions (0.5, 0.5). The obtained numerical results are shown in Figure 13. From this figure, we observe that the new chemical system (1) exhibits various bifurcations such as period-doubling and reverse period-doubling bifurcations, period windows, period-m bubbles and reverse period-m bubbles, antimonotonicity, intermittency, symmetry breaking, and symmetry restoring. In addition, period-9 orbit route to chaos and period-m bubbles route to chaos occur in the system. On the contrary, we also observe merging of chaotic regions between the forward and reverse period-doubling sequences.

When we use the external excitation frequency, Ω, as the control parameter, with $f = 1.8$, $p = 0.005$, and $\alpha_0 = -0.0193$, the new nonlinear chemical oscillator under the study displays a period-3 route to chaos, period-1 route to chaos, periodic windows, reverse period doubling, symmetry breaking and symmetry restoring, bistable chaotic oscillations, and various coexisting behaviors of symmetric and asymmetric attractors (see Figure 14). Figure 15 illustrates the different attractors predicted by bifurcation diagrams of Figure 14 for several different values of Ω. Through this figure, we notice that our new chemical model presents several bistable symmetric and asymmetric attractors of different topologies and remarkable routes to chaos. We can conclude that the new nonlinear parametric oscillator under consideration displays a rich variety of dynamical behaviors with unusual transitions to chaos.

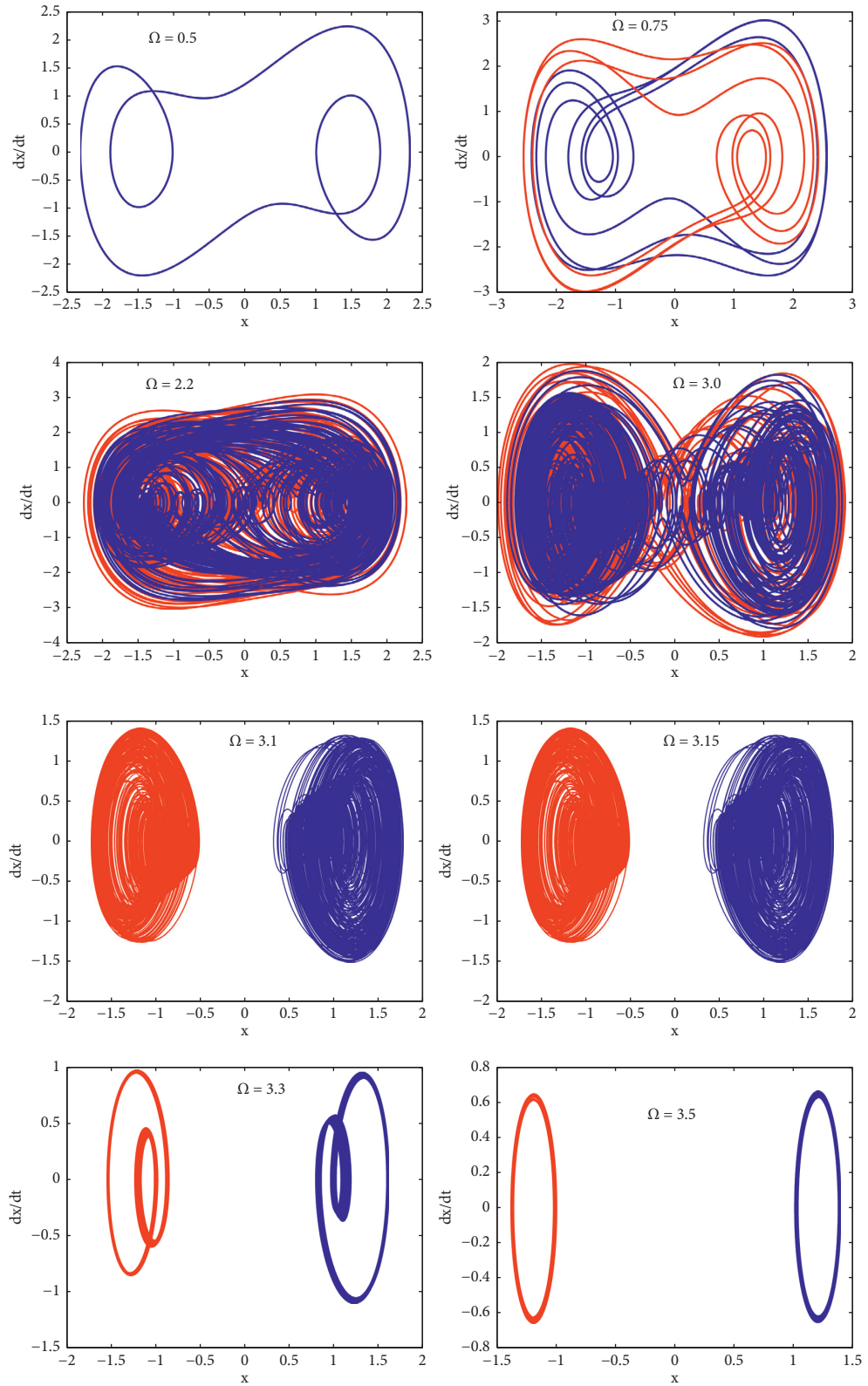

Figure 15: Various phase portraits illustrating monostability, bistability, and coexistence of attractors for different values of Ω with the parameters of Figure 13.

4. Conclusions

This study deals with nonlinear dynamics of Briggs–Rauscher reaction system modeled by a new nonlinear parametric oscillator. The Melnikov method is used to derive the condition of the appearance of horseshoe chaos in a new nonlinear parametric chemical oscillator in the cases, where $\Omega = \omega$ and $\Omega \neq \omega$. The numerical simulations realized confirm the obtained analytical predictions. On the contrary, the complex dynamics of the new nonlinear parametric chemical oscillator (1) is investigated numerically by using the fourth-order Runge–Kutta algorithm. The obtained results show that the parametric parameter p also induces in the new chemical parametric system and the symmetry breaking phenomenon and removes the symmetry restoring crisis phenomenon when p increases. Note that the new nonlinear parametric chemical system presents bistability phenomenon and coexisting behaviors of asymmetric attractors in the case $\Omega = \omega$. Moreover, it is found that three chaotic attractors of different topologies coexist for $f = 7.9$. As ω/Ω is irrational, the geometrical shape of attractors has completely changed. In addition, the symmetry restoring crisis phenomenon disappears in the new chemical system under the study. The dynamical behavior of our new chemical system becomes rich when ω/Ω is rational. In this case, the coexisting behavior of symmetric and asymmetric attractor appears in the system as well as the bistability phenomenon. Furthermore, for $f = 2.6$ and $f = 8.75$, multiple coexisting attractors take place in the system. As p varies in this case of oscillation, the new chemical parametric system (1) exhibits various bifurcations such as symmetry breaking and symmetry restoring, period doubling and reverse period doubling, period windows, intermittency, period-m bubbles and reverse period-m bubbles, intermittency, and antimonotonicity. In addition, period-9 orbit route chaos and period-m bubbles transition to chaos occur in the system as well as remerging chaotic band attractors. When Ω is used as control parameter, the new nonlinear chemical oscillator displays also various symmetric and asymmetric bistable attractors. Moreover, symmetry breaking, symmetry restoring, reverse period doubling, period-3 orbit route to chaos, and period-1 motion leading to chaos are obtained.

Appendix

A. Expression of $K_{i\in\{0,1,2,3\}}$

$$
\begin{aligned}
K_0 &= -\frac{4\mu\sigma^5}{15\alpha_3^2\delta^2}\left(1+x_0^2\right){}_2F_1\left(2,1;\frac{7}{2};\frac{1}{1-\nu^2}\right) \mp \frac{16\mu\sqrt{2}\sigma^7 x_0}{105\alpha_3^3\delta^3}\,{}_2F_1\left(\frac{5}{2},\frac{3}{2};\frac{9}{2};\frac{1}{1-\nu^2}\right)\\
&\quad -\frac{16\mu\sigma^9}{315\alpha_3^4\delta^4}\,{}_2F_1\left(3,2;\frac{11}{2};\frac{1}{1-\nu^2}\right),\\
K_2 &= -\frac{2\sqrt{2}\sigma\omega\pi\alpha_0}{\alpha_3\sqrt{x_0^2-\delta^2}}\,\frac{\sin\left((\omega/\sigma)\cosh^{-1}\left(x_0/\delta\right)\right)}{\sinh\left(\omega\pi/\sigma\right)} - \frac{2\sqrt{2}\omega\pi\alpha_1 x_0\,\sigma}{\alpha_3\sqrt{x_0^2-\delta^2}}\,\frac{\sin\left((\omega/\sigma)\cosh^{-1}\left(x_0/\delta\right)\right)}{\sinh\left(\omega\pi/\sigma\right)}\\
&\quad -\frac{2\alpha_1\,\sigma\omega\left(\sigma^2+\omega^2\right)\pi}{3\alpha_3^2\delta^2\sinh\left(\omega\pi/\sigma\right)}\,{}_2F_1\left(1+i\frac{\omega}{2\sigma},1-i\frac{\omega}{2\sigma};\frac{5}{2};\frac{1}{1-\nu^2}\right) - \frac{2\sqrt{2}\omega\pi\sigma x_0^3}{\sqrt{x_0^2-\delta^2}}\,\frac{\sin\left((\omega/\sigma)\cosh^{-1}\left(x_0/\delta\right)\right)}{\sinh\left(\omega\pi/\sigma\right)}\\
&\quad -\frac{2\sigma\omega x_0^2\left(\sigma^2+\omega^2\right)\pi}{\alpha_3\delta^2\,\sinh\left(\omega\pi/\sigma\right)}\,{}_2F_1\left(1+i\frac{\omega}{2\sigma},1-i\frac{\omega}{2\sigma};\frac{5}{2};\frac{1}{1-\nu^2}\right)\\
&\quad \mp\frac{2\sqrt{2}x_0\sigma\omega\left(4\sigma^2+\omega^2\right)\left(\sigma^2+\omega^2\right)\pi}{15\alpha_3^2\delta^3\sinh\left(\omega\pi/\sigma\right)}\,{}_2F_1\left(\frac{3}{2}+i\frac{\omega}{2\sigma},\frac{3}{2}-i\frac{\omega}{2\sigma};\frac{7}{2};\frac{1}{1-\nu^2}\right)\\
&\quad -\frac{\sigma\pi\omega\left(9\sigma^2+\omega^2\right)\left(4\sigma^2+\omega^2\right)\left(\sigma^2+\omega^2\right)}{315\alpha_3^3\delta^4\sinh\left(\omega\pi/\sigma\right)}\,{}_2F_1\left(2+i\frac{\omega}{2\sigma},2-i\frac{\omega}{2\sigma};\frac{9}{2};\frac{1}{1-\nu^2}\right),
\end{aligned}
\tag{A.1}
$$

with

$$\frac{1}{1-\nu^2} = 1 - \frac{x_0^2}{\delta^2},$$
$$K_3 = \frac{2\sqrt{2}\sigma\Omega\pi}{\alpha_3\sqrt{x_0^2-\delta^2}} \frac{\sin\left((\Omega/\sigma)\cosh^{-1}(x_0/\delta)\right)}{\sinh(\Omega\pi/\sigma)}. \quad \text{(A.2)}$$

Data Availability

All the data are included within the article.

Conflicts of Interest

The authors declare that there are no conflicts of interest regarding the publication of this paper.

References

[1] L. Cveticanin, *Strong Nonlinear Oscillators*, Springer, 2nd edition, 2018.

[2] S. Strogatz, *Nonlinear Dynamics and Chaos: With Applications to Physics, Biology, Chemistry, and Engineering*, Perseus Books, New York, NY, USA, 1994.

[3] A. H. Nayfeh and D. T. Mook, *Nonlinear Oscillations*, John Wiley & Sons, New York, NY, USA, 1995.

[4] M. Bayat, I. Pakar, and G. Domairry, "Recent developments of some asymptotic methods and their applications for nonlinear vibration equations in engineering problems: a review," *Latin American Journal of Solids and Structures*, vol. 9, no. 2, pp. 1–93, 2012.

[5] S. Fiori, "Nonlinear damped oscillators on Riemannian manifolds: numerical simulation," *Communications in Nonlinear Science and Numerical Simulation*, vol. 47, pp. 207–222, 2017.

[6] A. H. Nayfeh, *Perturbation Methods*, Wiley-VCH Verlag GmbH & Co.KGaA, 2004.

[7] M. Siewe Siewe, F. M. Moukam Kakmeni, C. Tchawoua, and P. Woafo, "Bifurcations and chaos in the triple-well φ^6 Van der Pol oscillator driven by external and parametric excitations," *Physica A: Statistical Mechanics and Its Applications*, vol. 357, no. 3-4, pp. 383–396, 2005.

[8] L. A. Hinvi, A. A. Koukpémèdji, V. A. Monwanou, C. H. Miwadinou, V. Kamdoum Tamba, and J. B. Chabi Orou, "Resonance, chaos and coexistence of attractors in a position dependent mass-driven Duffing-type oscillator," *Journal of the Korean Physical Society*, vol. 79, no. 8, pp. 755–771, 2021.

[9] Y. J. F. Kpomahou and J. A. Adéchinan, "Nonlinear dynamics and active control in a Liénard-type oscillator under parametric and external periodic excitations," *American Journal of Computational and Applied Mathematics*, vol. 10, no. 2, pp. 48–61, 2020.

[10] T. K. Dutta and P. K. Prajapati, "Some dynamical properties of the Duffing equation," *International Journal of Engineering Research & Technologies*, vol. 5, no. 12, pp. 500–503, 2016.

[11] I. R. Epstein and J. A. Pojman, *An Introduction to Nonlinear Chemical Dynamics*, Oxford University Press, Oxford, UK, 1998.

[12] A. B. Cambel, *An Introduction to Nonlinear Chemical Dynamics*, Academic Press, Cambridge, MA, USA, 1993.

[13] I. R. Epstein and K. Showalter, "Nonlinear chemical dynamics: oscillations, patterns, and chaos," *The Journal of Physical Chemistry*, vol. 100, no. 31, pp. 13132–13147, 1996.

[14] K. Showalter and I. R. Epstein, "From chemical systems to systems chemistry: patterns in space and time," *Chaos: An Interdisciplinary Journal of Nonlinear Science*, vol. 25, no. 9, pp. 97613–97621, 2015.

[15] M. A. Budroni, I. Calabrese, Y. Miele, M. Rustici, N. Marchettini, and F. Rossi, "Control of chemical chaos through medium viscosity in a batch ferroin-catalysed Belousov-Zhabotinsky reaction," *Physical Chemistry Chemical Physics*, vol. 19, no. 48, pp. 32235–32241, 2017.

[16] R. J. Field, "Chaos in the belousov-zhabotinsky reaction," *Modern Physics Letters B*, vol. 29, no. 34, pp. 1–39, 2015.

[17] V. Voorsluijs, I. G. Kevrekidis, and Y. De decker, "Nonlinear behavior and fluctuation-induced dynamics in the photosensitive Belousov-Zhabotinsky reaction," *Physical Chemistry Chemical Physics*, vol. 19, no. 33, pp. 22528–22537, 2017.

[18] Y.-N. Li, H. Song, Z.-S. Cai et al., "New chaotic behavior and its effective control in Belousov–Zhabotinsky reaction," *Canadian Journal of Chemistry*, vol. 79, no. 1, pp. 29–34, 2001.

[19] A. Cassani, A. Monteverde, and M. Piumetti, "Belousov-Zhabotinsky type reactions: the non-linear behavior of chemical systems," *Journal of Mathematical Chemistry*, vol. 59, no. 3, pp. 792–826, 2021.

[20] J. A. Adéchinan, Y. J. F. Kpomahou, C. H. Miwadinou, and L. A. Hinvi, "Dynamics and active control of chemical oscillations modeled as a forced generalized Rayleigh oscillator with asymmetric potential," *International Journal of Basic and Applied Sciences*, vol. 10, no. 2, pp. 20–31, 2021.

[21] A. V. Monwanou, A. A. Koukpémèdji, C. Aïnamon, P. R. Nwagoun Tuwa, C. H. Miwadinou, and J. B. Chabi Orou, "Nonlinear dynamics in a chemical reaction under an amplitude-modulated excitation: hysteresis, vibrational, resonance, multistability, and chaos," *Complexity*, vol. 2021, Article ID 8823458, 16 pages, 2021.

[22] D. L. Olabodé, C. H. Miwadinou, A. V. Monwanou, and J. B. Orou, "Horseshoes chaos and its passive control in nonlinear chemical dynamics," *Physica Scripta*, vol. 93, no. 8, pp. 1–19, 2018.

[23] D. L. Olabodé, C. H. Miwadinou, A. Monwanou, and J. B. C. Orou, "Effects of passive hydrodynamics force on harmonic and chaotic oscillations in dissipative nonlinear chemical dynamics," *Physica D*, vol. 386-387, pp. 49–59, 2019.

[24] S. Ghosh and D. S. Ray, "Liénard-type chemical oscillator," *The European Physical Journal B*, vol. 87, no. 65, pp. 1–7, 2014.

[25] H. Binous and A. Bellagi, "Introducing nonlinear dynamics to chemical and biochemical engineering graduate students using mathematica," *Computer Applications in Engineering Education*, vol. 27, no. 1, pp. 1–19, 2018.

[26] A. Shabunin, V. Astakhov, V. Demidov et al., "Modeling chemical reactions by forced limit-cycle oscillator: synchronization phenomena and transition to chaos," *Chaos, Solitons & Fractals*, vol. 15, no. 2, pp. 395–405, 2003.

[27] C. H. Miwadinou, A. V. Monwanou, J. Yovogan, L. A. Hinvi, P. R. Nwagoum Tuwa, and J. B. Chabi Orou, "Modeling nonlinear dissipative chemical dynamics by a forced modified Van der Pol-Duffing oscillator with asymmetric potential: chaotic behaviors predictions," *Chinese Journal of Physics*, vol. 56, no. 3, pp. 1089–1104, 2018.

[28] M. V. S. Meenakshi, S. Athisayanathan, V. Chinnathambi, and S. Rajasekar, "Homoclinic Bifurcation in a parametrically driven nonlinearly damped Duffing-vander Pol oscillator," *International Journal of Advances in Applied Mathematics and Mechanics*, vol. 6, no. 1, pp. 10–20, 2018.

[29] C. Si-yu and T. Jin-yuan, "Study on a new nonlinear parametric excitation equation: stability and bifurcation," *Journal of Sound and Vibration*, vol. 318, no. 4-5, pp. 1109–1118, 2008.

[30] J. Y. Tang, S. Y. Chen, and J. Zhong, "A improved nonlinear model of a spur gear pair system," *Engineering Mechanics*, vol. 1, no. 25, pp. 217–223, 2008.
[31] F. Sagués and I. R. Epstein, *Nonlinear dynamics," Dalton Transactions*, vol. 34, no. 7, pp. 1201–1217, 2003.
[32] Z. Wang, H. R. Abdolmohammadi, F. E. Alsaadi, T. Hayat, and V.-T. Pham, "A new oscillator with infinite coexisting asymmetric attractors," *Chaos, Solitons & Fractals*, vol. 110, no. C, pp. 252–258, 2018.
[33] K. Sun, A. D.-L. D. Li-kun, Y. Dong, H. Wang, and K. Zhong, "Multiple coexisting attractors and hysteresis in the generalized Ueda oscillator," *Mathematical Problems in Engineering*, vol. 2013, Article ID 256092, 7 pages, 2013.
[34] K. Zang, M. D. Vijayakumar, S. S. Jamal et al., "A novel megastable oscillator with a strange structure of coexisting attractors: design, analysis and FPGA implementation," *Complexity*, vol. 2021, Article ID 2594965, 11 pages, 2021.
[35] B. Deruni, A. S. Hacinliyan, E. Kandiran et al., "Coexisting attractors and bubbling route to chaos in modified coupled Duffing oscillators," *Australian Journal of Mathematical Analysis and Applications*, vol. 18, no. 1, pp. 1–13, 2021.
[36] M. Yan and H. Xu, "A chaotic system with a nonlinear term and multiple coexistence attractors," *The European Physical Journal Plus*, vol. 135, no. 6, pp. 1–9, 2020.
[37] N. Wang, G. Zhang, and H. Bao, "Bursting oscillations and coexisting attractors in a simple memristor-capacitor-based chaotic circuit," *Nonlinear Dynamics*, vol. 97, no. 4, pp. 1477–1494, 2019.
[38] N. Wang, G. Zhang, and N. V. K. H. Bao, "Hidden attractors and multistability in a modified Chua's circuit," *Communications in Nonlinear Science and Numerical Simulation*, vol. 92, Article ID 105494, 2021.
[39] B. Bao, T. Jiang, Q. Xu, M. Chen, H. Wu, and Y. Hu, "Coexisting infinitely many attractors in active band-pass filter-based memristive circuit," *Nonlinear Dynamics*, vol. 86, no. 3, pp. 1711–1723, 2016.
[40] T. S. Briggs and W. C. Rauscher, "An oscillating iodine clock," *Journal of Chemical Education*, vol. 50, no. 7, p. 496, 1973.
[41] J. Boissonade and P. De Kepper, "Transitions from bistability to limit cycle oscillations. Theoretical Analysis and experimental evidence in an open chemical system," *The Journal of Physical Chemistry*, vol. 84, no. 5, pp. 501–506, 1980.
[42] Y. J. F. Kpomahou, L. A. Hinvi, J. A. Adechinan, and C. H. Miwadinou, "Chaotic dynamic of a Mixed Rayleigh-Liénard oscillator driven by parametric damping and external excitations," *Complexity*, vol. 2021, Article ID 6631094, 18 pages, 2021.
[43] I. S. Gradshteyn and I. M. Ryzhik, *Table of Integrals, Series, and Products*, Academic Press, New York, NY, USA, 2007.
[44] X. Chen, X. Fu, X. Fu, and Z. Jing, "Chaos control in a special pendulum system for ultra-subharmonic resonance," *Discrete & Continuous Dynamical Systems-B*, vol. 26, no. 2, pp. 847–860, 2021.
[45] B. R. Chacon, "Melnikov method approach to control of homoclinic/heteroclinic chaos by weak harmonic excitations," *Philosophical Transactions of the Royal Society A*, vol. 364, pp. 2335–2351, 2012.